A data-driven framework for comprehensive identification of operational wind turbines under uncertainty

S. Bogoevska[1], M. Spiridonakos[2], E. Chatzi[2], E. D. Jovanoska[1],R. Höffer[3]
[1] University Ss. Cyril and Methodius, Faculty of Civil Engineering
Partizanski Odredi 24 1000, Skopje, Republic of Macedonia
e-mail: **simona.bogoevska@gf.ukim.edu.mk**

[2] ETH Zürich, Department of Civil, Environmental and Geomatic Engineering
Stefano-Franscini-Platz 5 8093, Zurich, Switzerland

[3] Ruhr-University Bochum, Faculty of Civil and Environmental Engineering
Universitätsstraße 150 44801, Bochum, Germany

Abstract
In order to capture the characteristic short- and long-term variability of Wind Turbine (WT) systems, it is crucial to incorporate the uncertainties related to various sources within mathematical prediction models. A data-driven framework able to link the temporal variability characterizing the system with the random evolution of environmental and operational parameters affecting the system is applied on long-term data collected from a real operating WT structure located in Dortmund, Germany. Particular focus placed us on the configuration of the input variable set, namely the evaluation of Polynomial Chaos Expansion (PCE) model estimates for the case of blind and reasoned source selection. The overviewed framework leads to effective reduction of the input set dimension facilitating the implementation of the proposed approach in an automated fashion. The developed data-driven tool proves robust in quantifying the uncertainty linked to the evolution of the structural dynamics throughout the structure's operational envelope.

1 Introduction

Structural Health Monitoring (SHM) based solutions enable the extraction of comprehensive structural dynamics models of operating WT structures, under the condition that challenges attributed to stochasticity, complexity and limited knowledge of the conditions may be successfully bridged. The intrinsic stochasticity of operating WT structures may be largely attributed to limited knowledge of the inputs (alternating aerodynamics loads), the complexity related to the interacting subsystems of the structure (namely the rotating blades, moving yaw mechanism, and pitch angle changes), varying operational regimes and environmental factors, as well as the typical uncertainties related to complex and unique to the location soil-structure interaction effects, modeling errors, incomplete and imperfect sensor data [1].

The vast number of already developed and laboratory verified SHM assessment tools in the field, as well as recently emerged technologies have channeled the focus of the research community towards holistic and automated SHM strategies, capable of early damage detection, diagnostics and prediction [2-5]. The process is further accelerated with WT infrastructure landing at the epicenter of Europe's strategic resource planning. The high demands for productivity and reduced downtime standards put in place by today's "renewable Europe" increase the necessity for efficient management of WTs [6].

However, when it comes to developing an efficient performance-based structural framework for an operating WT system the major difficulty is related to the benign structural changes linked to the changing operational regimes and varying environmental agents. Indeed, the time varying nature of WT structures and the misinterpretation of this variability oppose the effective operation of installed damage detection and intervention control systems by camouflaging the actual condition of the structure or by triggering false

alarms [7]. It then becomes evident that the commonly applied Operational Modal Analysis (OMA) set of methods, oriented towards linear time invariant systems, are no longer suitable and more refined schemes related to non-stationary systems need to be exploited [8, 9].

To alleviate the aforementioned conundrum, research studies in this field are generally following one of two streamlines: i) filtering out, or ii) merging environmental variables from/into models of measured vibration response. An approach based on filtering out the influence of environmental factors from estimated performance indices is applied in [10], where by analysis relying on the principal component analysis method the authors extract a structural health index of an operational 5 MW prototype wind turbine by removing temperature effects from selected natural frequency estimates.

Spiridonakos & Chatzi in [11,12] introduced and successfully applied the second approach via implementation of a bi-component SHM framework for the purpose of damage detection of the benchmark SHM project of the Z24-bridge in Switzerland. In [13] Spiridonakos *et al.* combined this framework with time varying autoregressive models for the purpose of developing a time-sensitive tool capable of tracking long-term variability of an actual operating WT tower located in Lübbenau, Germany. In a recent study in [14] the method was verified on an operating WT system in Dortmund, Germany, and delivered a robust model able to reproduce the one-month vibration response data with precision.

The main driver of the proposed strategy [12-14] relies on casting the problem in two separate temporal scales: a short-term time framework, which aims at accurately modeling the temporal variability charactering the system, while observing the structure as an isolated system, and a long-term time framework, which focuses on the tracking of the evolution of the variability in a longer time horizon, thus incorporating the effects of randomness of measured environmental data.

Following this approach, the research study presented herein will focus on evaluating the long-term tracking performance when the operational and environmental parameters are based on a) blind robust selection, or b) reasoned controlled selection. By inspection of the computational efficiency and empirical errors of the model estimates for both cases, the aspects of input data reduction and stability in case of automatized utilization are addressed, thus demonstrating the potential for incorporation within a holistic SHM damage detection framework, further extended via statistical hypothesis testing.

2 Framework description

The applied SHM framework aims to deliver statistical models encoded with a unique structural performance genetic code, in which the effects of the varying operational and environmental conditions are encrypted. The proposed data-driven strategy is two-sided. Firstly, employment of a parametric system identification technique, namely Smoothness Priors Time Varying Autoregressive Moving Average (SP-TARMA) model for the adequate capturing of the non-stationary short-term dynamics, in contrast to standard operational modal analysis methods adequate for structural responses closer to stationary. Secondly, adoption of a PCE probabilistic model for describing the uncertainty in the identified structural performance indicators originating from the stochasticity of operational and environmental data (Fig.1). This is achieved via projection of selected performance indicators, derived from the short-term dynamics (e.g. statistical moments of the SP-TARMA model residuals), onto the probability space of the influencing agents (wind loads, power, and temperature).

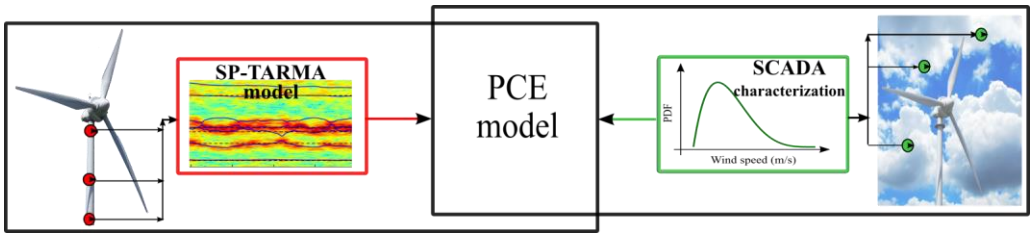

Figure 1: A conceptual overview of the bi-component framework

The changing dynamics of operating WTs calls for time sensitive modeling tools, capable of tracking the evolution of the identified response features. SP-TARMA models allow for a compact and parameterized formulation of a non-stationary signal, efficiently tracking temporal variability. The SP-TARMA model may be completely described by i) a model for the system response *y[t]* (Eq. 1), and ii) a model which "controls" the time evolution of the AR and MA (unknown) parameters of the first model (Eqs. 2 and 3), [15]:

$$y[t] + \sum_{i=1}^{n_a} a_i[t] \cdot y[t-i] = e[t] + \sum_{i=1}^{n_c} c_i[t] \cdot e[t-i], \quad e[t] \sim NID(0, \sigma_e^2[t]) \tag{1}$$

$$(1-B)^{\kappa} a_i[t] = w_{a_i}[t], \qquad w_{a_i}[t] \sim \mathrm{NID}(0, \sigma_{w_a}^2[t]) \tag{2}$$

$$(1-B)^{\kappa} c_i[t] = w_{c_i}[t], \qquad w_{c_i}[t] \sim \mathrm{NID}(0, \sigma_{w_c}^2[t]) \tag{3}$$

where *t* designates discrete time (with $i = 1,2,\dots,N$) of the observed nonstationary signal $y[t]$, $e[t]$ is the residual sequence (i.e., the unmodeled part of the signal, assumed to be normally identically distributed with zero mean and time-varying variance $e[t] \sim NID(0, \sigma_e^2[t])$) and $a_i[t]$, $c_i[t]$ designate the time-varying AR and MA parameters respectively, for an AR/MA order equal to *n*. B is the backshift operator ($B^k x[t] = x[t-k]$), κ designates the difference equation order, and $w_i[t]$ zero-mean, Gaussian sequences with time-dependent variance, uncorrelated, mutually uncorrelated and also uncrosscorrelated with $e[t]$.

For a given set of values of the three user-defined parameters, i.e., the AR/MA order *n*, the ratio of the residual variances $\nu = \sigma_w^2[t]/\sigma_e^2[t]$, and the order of the stochastic difference equations κ, the model is fitted to the actual structural response. A tuning of the values (n, ν, κ) , usually supported by statistical based "penalty" approaches, which hinder overfitting of the modeled signal [15], ensures a well-fitted model. The parameter estimation problem (Eqs. 1-3) is then solved via a Kalman Filter, aided by an Extended Least Squares-like algorithm in order to circumvent the nonlinear formulation, which is typical for the SP-TARMA full case [13].

For delivering the relationship between outputs (structural response estimates) and inputs (environmental and operational loads) of the system, the problem is further cast in the probability domain. For an assumed system S, the PCE generates a mathematical expansion of the model's random output variable *Y* on multivariate polynomial chaos basis functions, appropriately related to the model's random input data vector Ξ.

More specifically, if we assume the system $Y = S(\Xi)$ is comprised of *M* random input parameters represented by independent random variables, e.g. measured wind velocities and temperature values, gathered in the random vector Ξ of prescribed joint Probability Density Function (PDF) $p_{\Xi}(\xi)$, and the output variable is of finite variance, the PCE model assumes the form [16]:

$$Y = \mathrm{S}(\boldsymbol{\Xi}) = \sum_{\boldsymbol{d} \in \mathrm{N}^M} \theta_{\boldsymbol{d}} \varphi_{\boldsymbol{d}}(\boldsymbol{\Xi}) \tag{4}$$

where θ_d are unknown deterministic coefficients of projection, and d is the vector of multi-indices of the multivariate polynomial basis with total maximum degree $\left|\boldsymbol{d}_j\right| = \sum_{m=1}^{M} d_{j,m} \le P$ for every single index j. In this case, the number of terms in Eq. (4) is equal to:

$$p = \frac{(M+P)!}{M!P!} \tag{5}$$

where *M* designates the number of random variables and *P* denotes maximum basis degree.

The multivariate PC basis functions $\varphi_d(\Xi)$ are constructed through tensor products of the corresponding univariate functions, chosen in accordance to the PDF of the random input variables $p_{\Xi}(\xi)$, and thus straightforwardly associated to a well-known family of orthogonal polynomials [13]. Finally, the truncated

PCE model to the first p terms yields a finite parameter vector θ_d which may be estimated by solving Eq. (4) in a least squares sense.

3 Application case: operating WT structure

3.1 Description of the structure

The SHM bi-component framework is presently applied on an actual WT structure. The monitored structure is a 65m high real WT under operation (Fig.2), located in the vicinity of Dortmund, Germany. An extensive monitoring system has been installed to continuously record structural response (ambient vibration acceleration and displacement), environmental (wind velocity and direction, ambient and structural temperature) and operational (rotor velocity, power production, yaw angle and pitch angle changes) data of the WT structure for a period of four years, from October 2010 to October 2013. The output-only information is monitored by means of triaxial accelerometers (PCB-3713D1FD3G MEMS sensors). All aforementioned parameters are recorded at a sampling frequency of 100 Hz in hour-long data sets, during the complete monitoring period. A more detailed overview of the complete acquisition system can be found in [17].

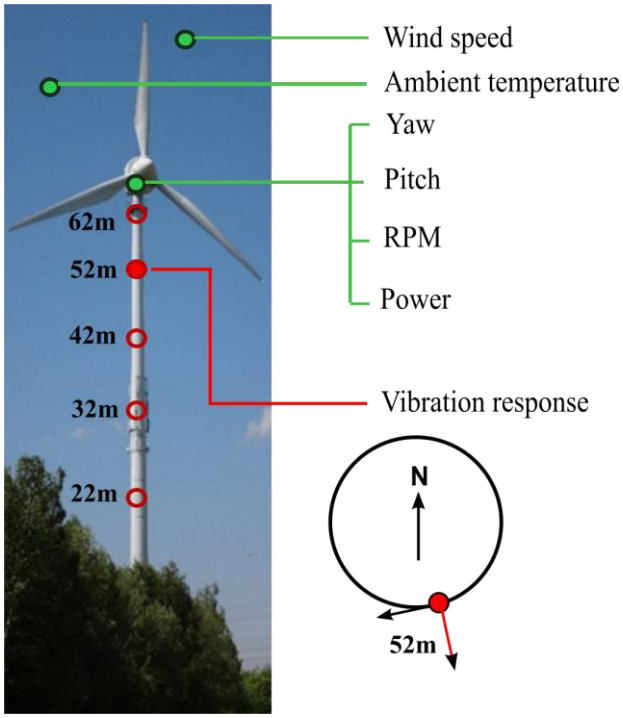

Power	500 kW
Height of the rotor center	65 m
Length of blade (3 total)	19.13 m
Rotor speed	18-36 rpm
Blade material	GRP
Tower material	steel
Construction year	1997

Figure 2: Schematic overview of measured data (left), WT structure characteristics (right)

3.2. Short-term framework

For the purposes of the SP-TARMA simulation, the one-hour acceleration time histories corresponding to normal operating conditions were low-pass filtered and down-sampled to 12.5 Hz (cutoff frequency at 6 Hz) and observed as 10-min long data sets [marked red in (Fig.2)]. The selected complete one-month period (June 2013) resulted in 4218 10-min long datasets. After a preliminary tuning phase the data sets were processed in an automated fashion within the short-term framework.

The tracking of the frequency evolution for a fitted SP-TARMA model (n_a=18, n_c=18, κ=1, ν=0.0001) in contrast to an overfitted one (n_a=18, n_c=18, κ=1, ν=0.001) is presented in Fig. 3. For comparison, spectrograms (Short Time Fourier Transform; Hamming data window; NFFT = 512; overlap 98%) are plotted in the background as well.

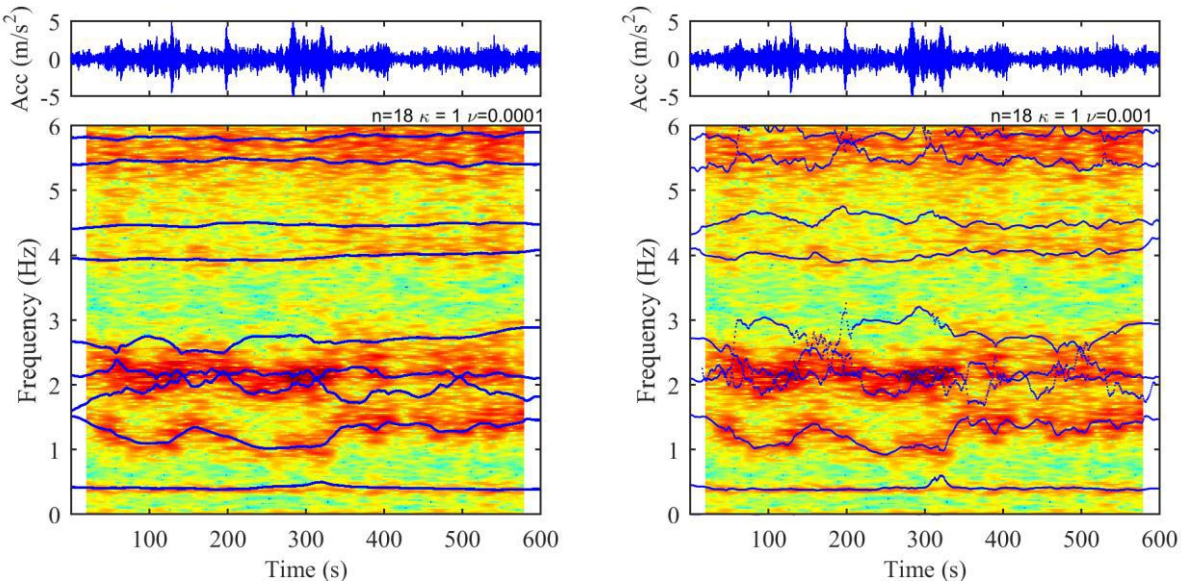

Figure 3: SP-TARMA estimates (spectrogram in the background): fitted (left) and overfitted (right)

3.3 Long-term framework

Before utilizing the long-term framework the appropriate operational/environmental parameters have to be carefully selected. The theoretical prerequisite for building a PCE model is utilization of independent random input variables. However, in case of practical applications involving measured physical quantities, this is an uncommon scenario. In this context, for the current case study of the operating WT structure the PCE model performance is tested for the following two cases of input variables: i) directly employed SCADA parameters with weak linear correlation, ii) correlated SCADA parameters which are transformed before employment to independent variables with negligible correlation.

3.3.1 Weakly correlated input data

For the case of weakly correlated variables, the 10 minute averages of selected SCADA parameters, corresponding to the 4218 acceleration measurements (utilized for the SP-TARMA modeling), are plotted in Fig. 4 (left plot). In the right plot of the same figure the correlation plots for each pair of chosen input variables is presented. The selected pairs are correlated with the highest negative Pearson correlation coefficient equal to -0.313. For the purpose of constructing the random vector Ξ of prescribed joint PDFs $p_{\Xi}(\xi)$, the input variables are further transformed into uniformly distributed variables via use of the non-parametrically estimated cumulative distribution functions.

As a last step, the SP-TARMA model output variables and the PDFs of the measured operational input data are fed into the PCE (long-term) framework. The standard deviation (std) of the SP-TARMA (18, 18, 1, 0.0001) residuals for the 10 minute intervals are selected as the PCE output parameter. In accordance with the uniform PDFs of the input data, the Legendre polynomials are selected as the PC functional basis [13].

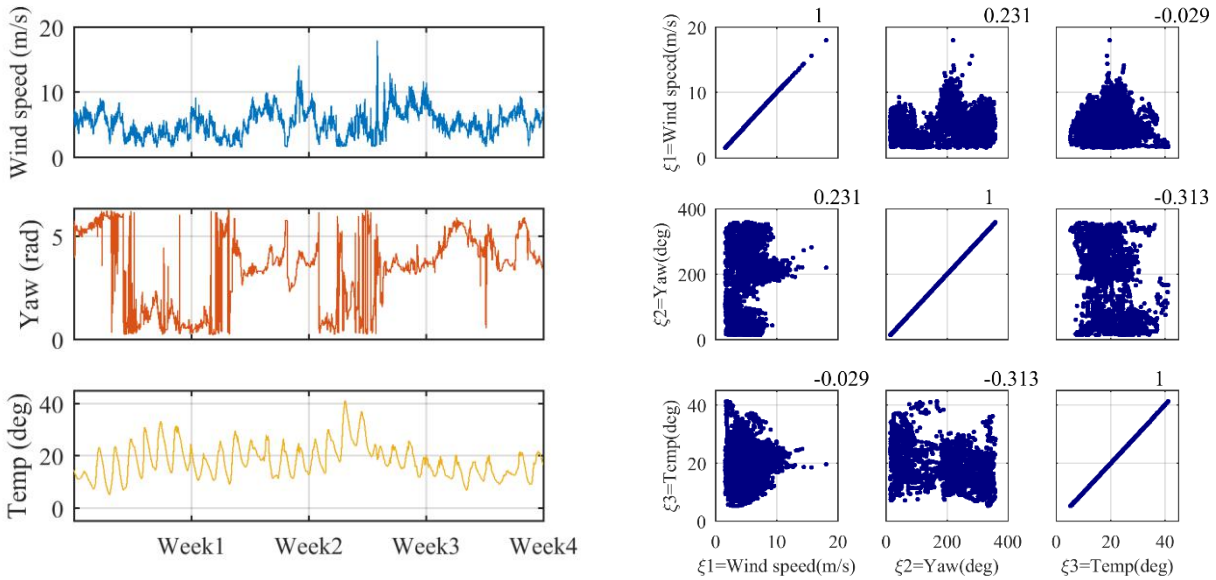

Figure 4: Left: Time-history plots of selected PCE input variables, Right: Scatter plots of selected PCE input variables with estimated Pearson correlation coefficient

The std of the residuals for each dataset and the PCE model estimates for the maximum polynomial order set equal to five are plotted in Fig. 5. The total data sets, which correspond to the four weeks of measurements, are divided into a three-week estimation period and a one-week validation period. The PCE errors are plotted in the lower part of the figure, along with the corresponding 95% confidence intervals calculated for the fitted Gaussian distribution of the estimation set errors. It may be observed that the obtained PCE model is capable of simulating the std(e) output variable with very good accuracy, and the model residual falls within the 95% confidence intervals for both sets.

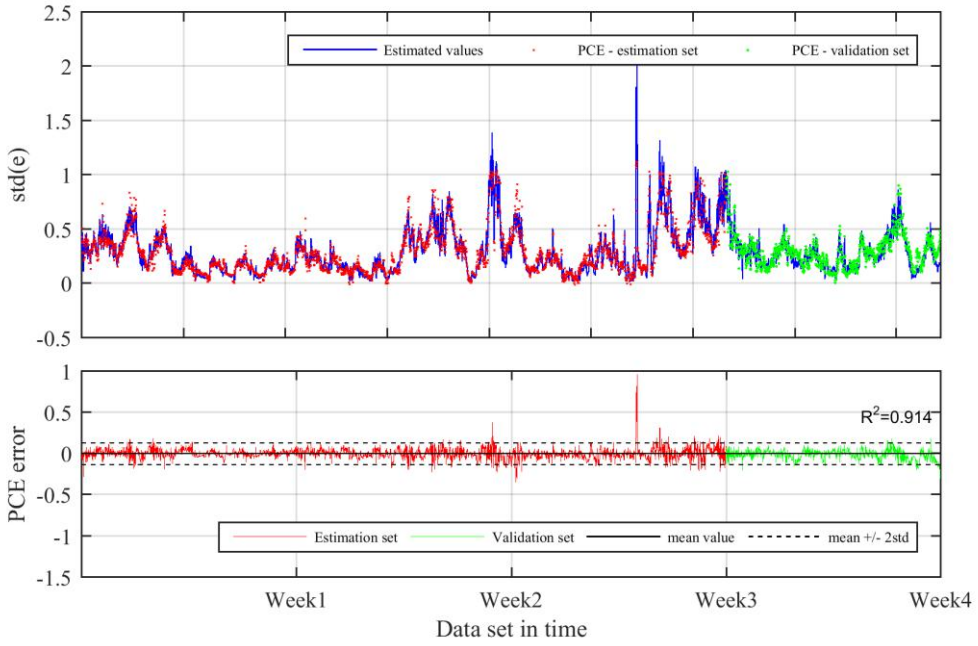

Figure 5: Up: PCE output estimates for weakly correlated input variables, Bottom: PCE error with 95% confidence intervals

An advantage of the direct employment of uncorrelated (weakly correlated) input parameters is the possibility of straightforward calculation of the PCE-based Sobol' indices. Sobol' indices are obtained as a sum of squares of the PC coefficients and represent the fraction of the total variance of the model output that can be attributed to each input variable or combinations of variables [18]. In Fig. 6 the estimated Sobol' first and second order indices for the estimation set (3163 data sets) of the PCE model (Fig. 5) are plotted. The highest index of 0.92 reveals that the variance of the modeled output parameter may mostly be attributed to the S1 index, directly related to the measured wind speed. Hence, the sensitivity analysis via post processing of estimated PC coefficients might contribute to reduction of the number of input data parameters, leading to higher computational efficiency (Fig. 7 right plot). In Fig. 7 (left plot) the PCE estimated std(e) for the case of three and one input parameter (wind speed) is presented. The number of PC terms for the case of one input variable reduces from p=56 to p=6, with a 2% difference in the estimated value of the R^2 coefficient of determination, usually applied as an error estimator [19].

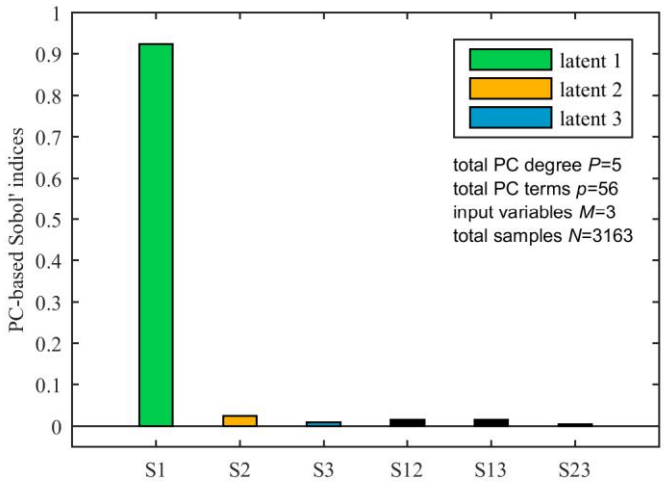

Figure 6: Sensitivity analysis: PCE-based Sobol' indices [S1=0.92, S2=0.02, S3=0.009]

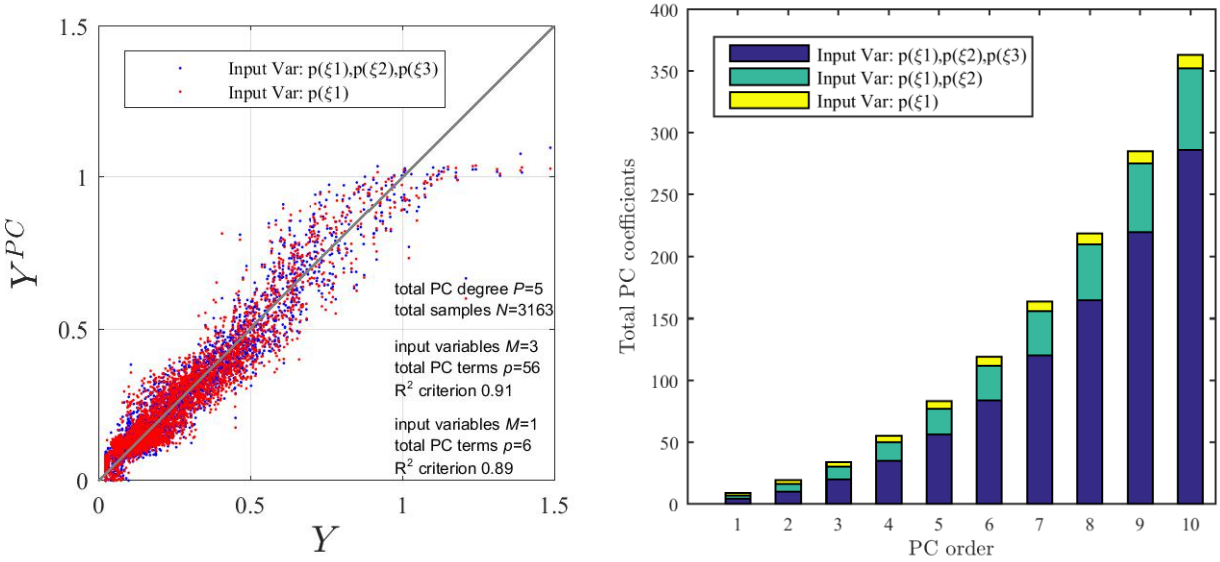

Figure 7: Left: PCE output estimates vs SP-TARMA std(e) for multivariate and univariate inputs; Right: Number of PC coefficients for three, two and one input variable for various PC orders

By further inspection of the R^2 coefficient of determination for the PCE estimates (training and validation sets), for the case of the complete set, and then reducing to two and one input variables only, we further assess the performance of the PCE model for the actual case (Fig. 8). A R^2 value close to 1 usually indicates a good accuracy of the model, whereas a R^2 close to zero characterizes a poor representation of the model response [19].

The plots for the estimation sets (full lines) of the three cases reveal the differences in achieved accuracy for the PC orders P=1 to 20. The case with two and one variable (red and blue filled line) have reached the maximum accuracy after the order P=12. The R^2 value for the case of three input parameters (black dashed line) destabilizes rapidly for the validation sets after an order P=6, while the univariate and bivariate model yield an almost constant accuracy for higher PC orders.

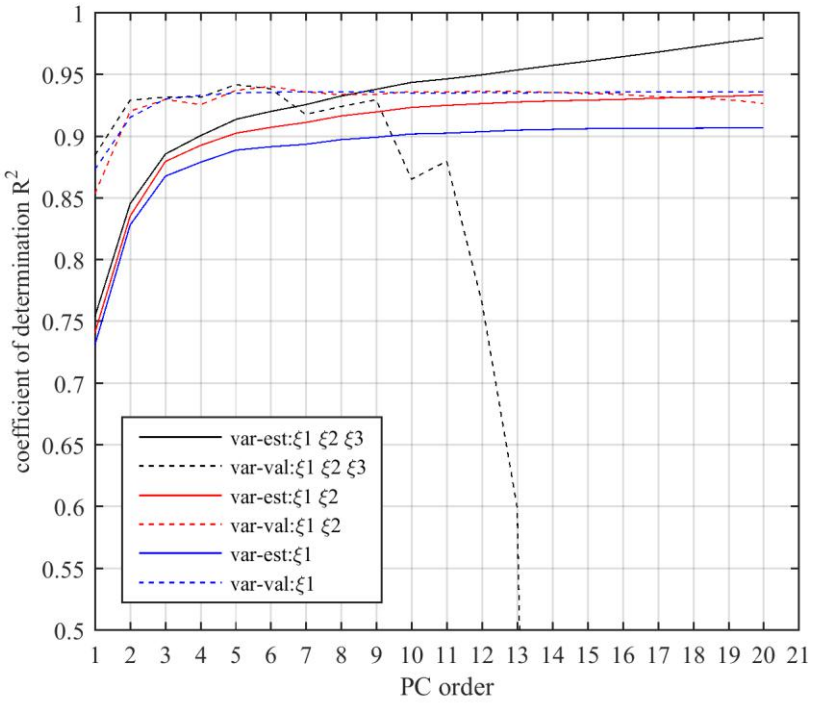

Figure 8: R^2 coefficient of determination for PCE model estimates for various PC orders and for multivariate and univariate inputs;

3.3.2 Moderate to highly correlated input data

The restriction in selecting a limited number of uncorrelated variables might result in omission of significant influences arising from other relevant input quantities. In this context, the PCE modeling is further tested for a broader set of correlated input variables.

In Fig. 9 the 10 minute averages of the second set of selected SCADA parameters, corresponding to the same time slot, are plotted. The Pearson correlation coefficient matrix for the six variables is presented in Table 1. As a first step related to the case of correlated inputs, the data is transformed to independent variables, thus satisfying the theoretical PCE method requirement. To this end, the Independent Component Analysis (ICA), a method capable of extracting independent unobservable (latent) variables by exploiting higher order statistics (maximizing non-Gaussianity of the unobserved sources) is applied [20]. For the purpose of illustration, the FASTICA algorithm is herein utilized for estimating three ICA-based variables (for estimated 3 Eigen values of the input data covariance matrix). The ICA estimates are further transformed into uniformly distributed variables via use of the non-parametrically estimated cumulative distribution functions (as for the previous case).

Fig. 10 shows the scatter plots and univariate (marginal) histograms of the variables with highest values of correlation coefficients (marked red in Tab.1) from the original SCADA set (before ICA) as well as from the newly estimated three ICA-based latent variables.

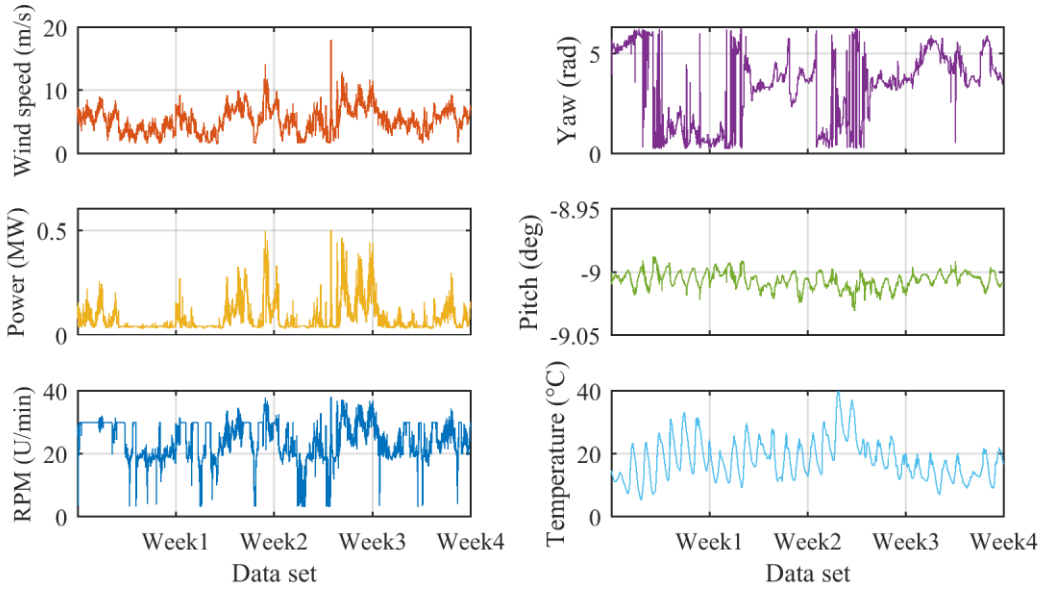

Figure 9: Time-history plots of measured SCADA variables – correlated set

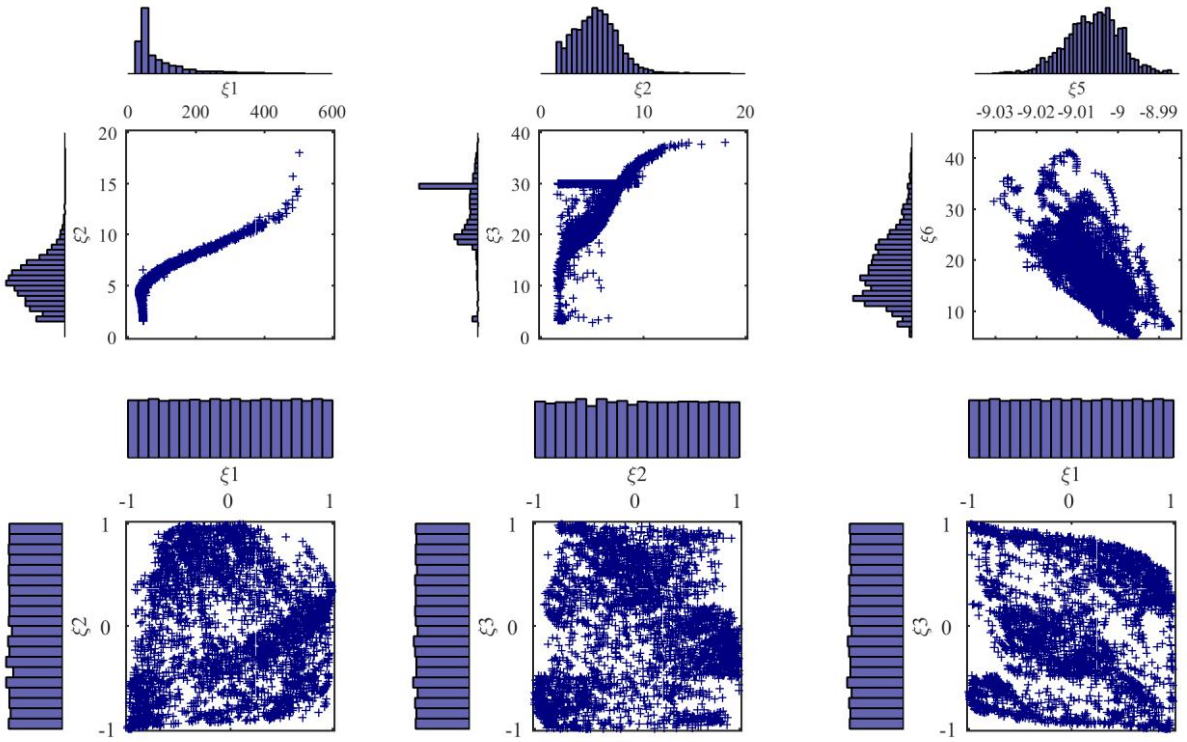

Figure 10: (Up) Scatter plots & marginal histograms of original input variables from Tab. 1
(Bottom) Scatter plots & marginal histograms of ICA-based input variables

	Power	WS	RPM	Yaw	Pitch	Temp.
Power	1	0.86	0.59	0.18	-0.56	0.06
WS	0.86	1	0.70	0.23	-0.55	-0.03
RPM	0.59	0.70	1	0.21	-0.09	-0.40
Yaw	0.18	0.23	0.21	1	-0.26	-0.31
Pitch	-0.56	-0.55	-0.09	-0.26	1	-0.65
Temp.	0.06	-0.03	-0.40	-0.31	-0.65	1

Table 1: Pearson correlation coefficient matrix

The implementation of the ICA algorithm has a twofold advantage: i) blind (robust and prone to automatization) seeding of measured input data variables, and ii) possibility for reduction of the number of input variables by the in-built whitening of the observed data (via eigen-value decomposition of the covariance matrix) [20]. On the other hand, the method dismisses the physical meaning of the estimated variables, thus disabling meaningful sensitivity analysis on output data of the PCE model.

The R^2 error estimator for the PCE model (estimation set), under application of a different number of Independent Components (IC) and Eigen Values (EV) extracted from the six original SCADA inputs, is presented in Fig. 11. For comparison, in the same figure (rightmost plot) the R^2 values for the Uncorrelated case of input Variables (UV) are plotted as well. The same graphs for the validation set are plotted in Fig. 12. An additional important criterion, particularly in the case of handling of a large database, is computational efficiency. Fig. 13 summarizes the relative computational time for the PCE model estimation in the case of a varying number of input parameters. In order to deliver an optimal PCE model performance for the actual case, the configuration of the PCE input variable set may be selected based on the criteria plotted in Figs. 11-13.

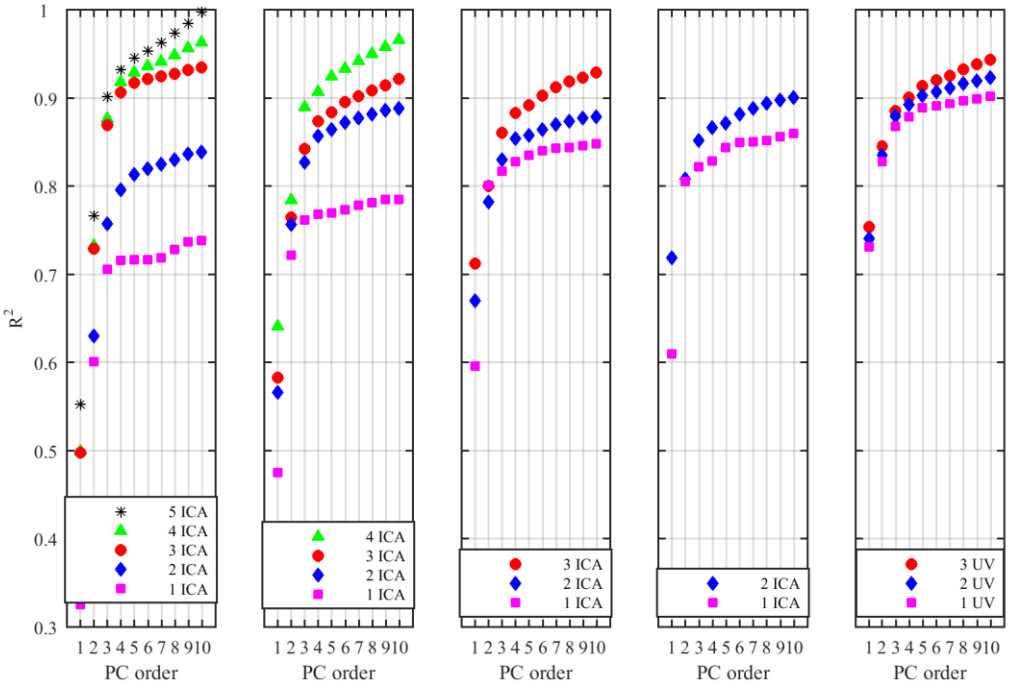

Figure 11: (from left to right) R^2 coefficient of determination for PCE outputs (estimation set) in case of: 5EV, 4EV,3EV,2EV, and the uncorrelated variables (UV) set

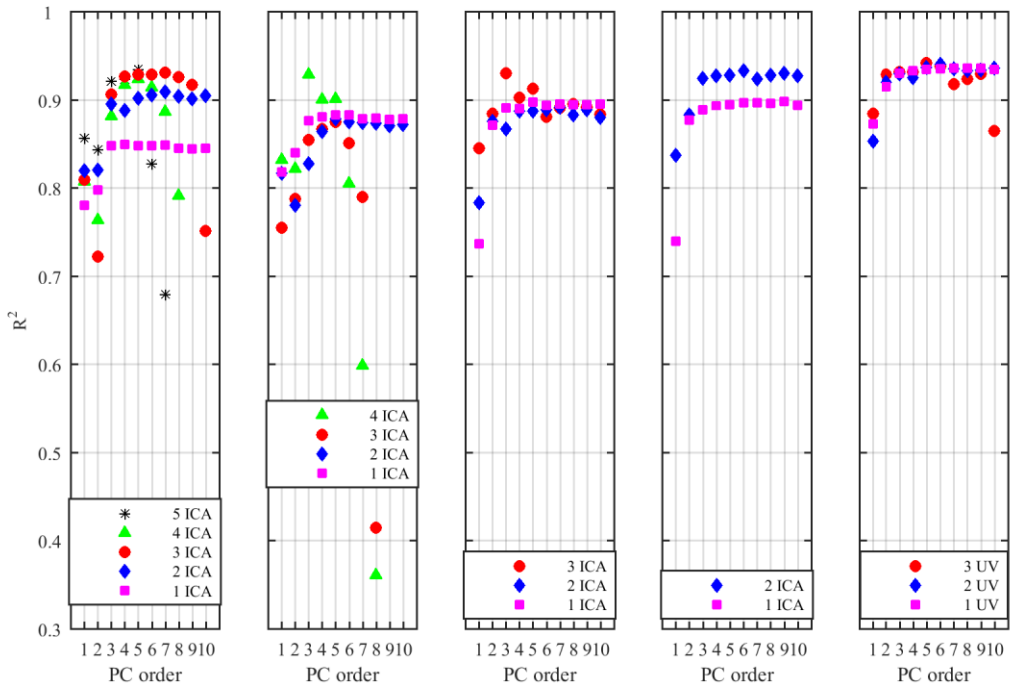

Figure 12: (from left to right) R^2 coefficient of determination for PCE outputs (validation set) in case of: 5EV, 4EV,3EV,2EV, and the uncorrelated variables (UV) set

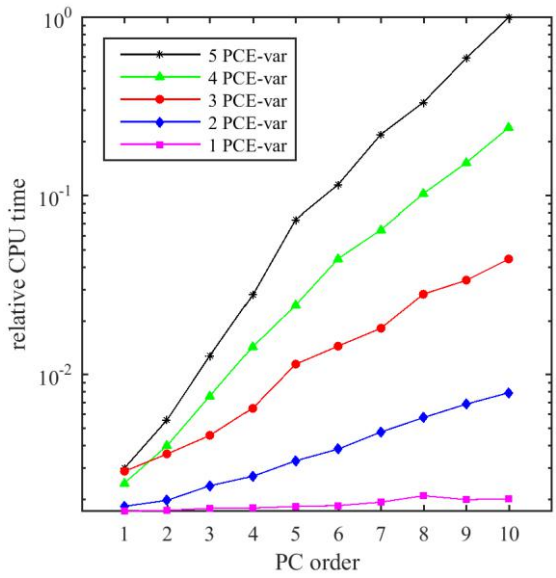

Figure 13: Relative computational time for the PCE model estimation with different number of inputs

For three different cases selected from Figs. 11-13 the PCE model estimates (Legendre polynomials, maximum polynomial order equal to five) are plotted in Fig. 14. The PCE model residuals fall within the 95% confidence intervals for all of the three sets, however differences in relation to the previously discussed selection criteria may be clearly observed.

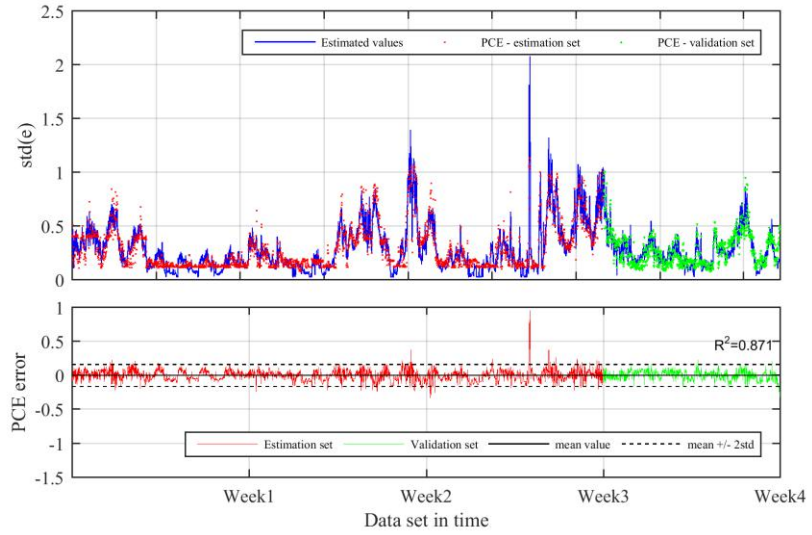

P=5
IC=2
EV=2

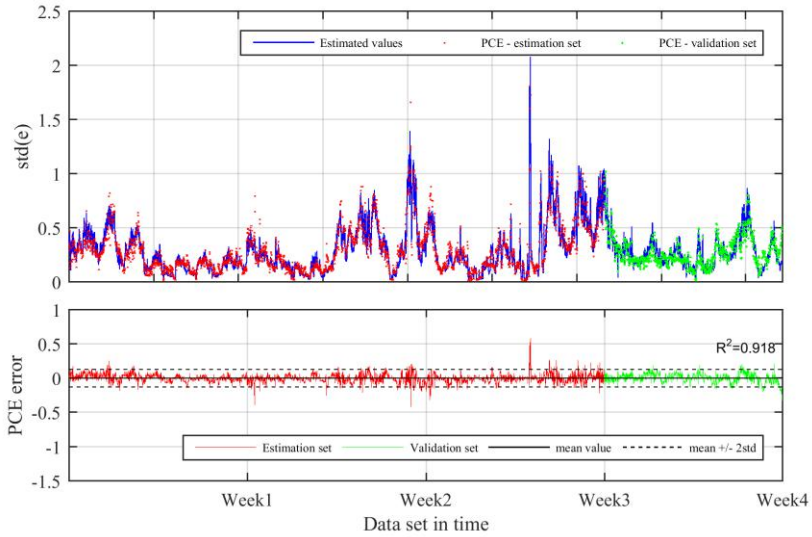

P=5
IC=3
EV=5

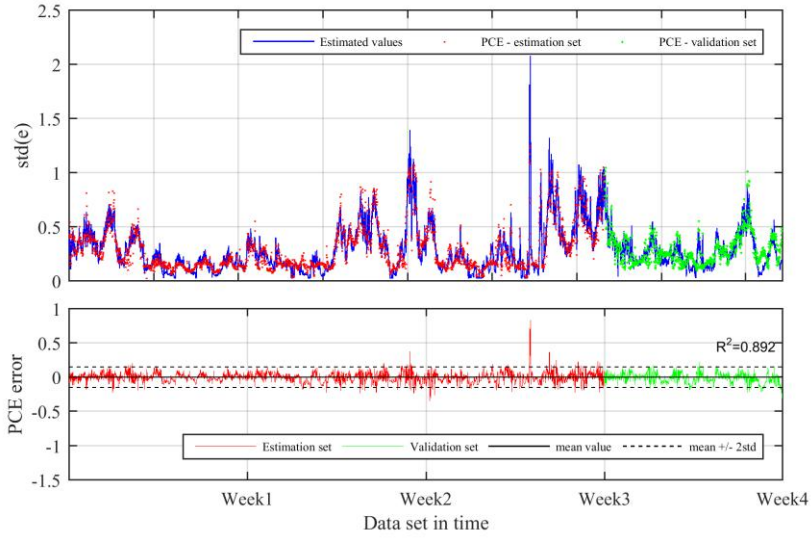

P=5
IC=3
EV=3

Figure 14: Comparison of PCE model estimates for three selected cases from Figs.11-13

Conclusions

Measured ambient vibration accelerations of an actual operating WT tower in Dortmund (Germany) along with environmental and operational data were exploited within a bi-component framework capable of delivering a robust time-sensitive model of the system response.

Successful implementation of the strategy renders a stochastic model of the synergy between output-only vibration response data and measured operational variables. The results verify the high potential of the proposed method for automated condition assessment of large real-world structures, operating in a wide range of conditions.

In this context, focus is herein shed on assessment of the performance of the long-term framework under different input dataset configurations, namely for blind and controlled selection of input parameters. The outcomes of the study demonstrate the effect on modeling errors, data reduction and computational efficiency, thus stressing the importance of proper selection criteria for an optimal autonomous tool, capable of tracking and diagnosing structural condition during the WT life-cycle.

References

[1] M. Ozbek, F. Meng , D. J. Rixen, *Challenges in testing and monitoring the in-operation vibration characteristics of wind turbines*, Mechanical Systems and Signal Processing, 41, pp. 649–666, 2013.

[2] C.C. Ciang, J.R. Lee, H.J. Bang, *Structural health monitoring for a wind turbine system: a review of damage detection methods*, Measurement Science and Technology, 19, pp. 1-20, 2008.

[3] Z. Hameed, Y. Hong, Y. Cho, S. Ahn, C. Song, *Condition monitoring and fault detection of wind turbines and related algorithms: a review*, Renewable and Sustainable Energy Reviews, 13, pp. 1-39, 2009.

[4] B. Yang, D. Sun, *Testing, inspecting and monitoring technologies for wind turbine blades: a survey*, Renewable and Sustainable Energy Reviews, 22, pp. 515-526, 2013.

[5] S. Thöns, *Monitoring based condition assessment of offshore wind turbine support structures*, PhD Thesis, Swiss Federal Institute of Technology Zurich, Institute of Structural Engineering, 2012.

[6] European commission, Energy road map 2050, 2011.

[7] H. Sohn, *Effects of environmental and operational variability on structural health monitoring*, Philosophical Transactions of the Royal Society A, 365, pp. 539-560, 2007.

[8] M. Spiridonakos, A. Poulimenos, S. Fassois, *Output-only identification and dynamic analysis of time-varying mechanical structures under random excitation: a comparative assessment of parametric methods*, Journal of Sound and Vibration, 329, pp. 768-785, 2010.

[9] L.D. Avendaño-Valencia, E.N. Chatzi, M.D. Spiridonakos, *Surrogate modeling of nonstationary systems with uncertain properties, Proceedings of The annual European Safety and Reliability Conference ESREL, Zurich, September, 2015.*

[10] W.H. Hu, S. Thöns, R. G. Rohrmann, S. Said, W. Rücker, *Vibration-based structural health monitoring of a wind turbine system Part II: environmental/operational effects on dynamic properties*, Engineering Structures, 89, pp. 273–290, 2015.

[11] M. Spiridonakos, E. Chatzi, *Polynomial chaos expansion models for SHM under environmental variability, Proceedings of 9th International Conference on Structural Dynamics, Porto, Portugal, 2014.*

[12] M. Spiridonakos, E. Chatzi, *Stochastic structural identification from vibrational and environmental data*, in Encyclopedia of Earthquake Engineering, M. Beer, E. Patelli, I.A. Kougioumtzoglou and I. S.-K. Au (Eds), Springer ISBN: 978-3-642-35344-4 (2014).

[13] M. Spiridonakos, Y. Ou, E. Chatzi, M. Romberg, *Wind turbines structural identification framework for the representation of both short- and long-term variability, Proceedings of 7th International Conference on Structural Health Monitoring of Intelligent Infrastructure, Torino, Italy, 2015*.

[14] S. Bogoevska, M. Spiridonakos, E. Chatzi, E.D.Jovanoska, R. Höffer, *A novel bi-component structural health monitoring strategy for deriving global models of operational wind turbines, Proceedings of the 8th European Workshop On Structural Health Monitoring, Bilbao, Spain, 2016.*

[15] M. Spiridonakos, A. Poulimenos, S. Fassois, *Output-only identification and dynamic analysis of time-varying mechanical structures under random excitation: a comparative assessment of parametric methods*, Journal of Sound and Vibration, 329, pp. 768-785, 2010.

[16] G. Blatman, B. Sudret, *An adaptive algorithm to build up sparse polynomial chaos expansions for stochastic finite element analysis*, Probabilistic Engineering Mechanics, 25, pp. 183-197, 2010.

[17] R. Höffer, S. Lachmann, D. Hartmann, S. Zimmermann, *Conceptual study on instrumentation and validation for displacement-based service strength checking of wind turbines, Proceedings of 14th International Conference on Computing in Civil and Building Engineering, Moscow, 2012*.

[18] B. Sudret, *Global sensitivity analysis using polynomial chaos expansion*, Reliability Engineering and System Safety**,** 93(7), pp. 964-979 , 2008.

[19] Y. Caniou, *Global sensitivity analysis for nested and multiscale modelling*, PhD Thesis, Blaise Pascal University – Clermont II , France , 2012.

[20] A. Hyvärinen, E. Oja, *Independent component analysis: algorithms and applications*, Neural Networks, Vol. 13, pp. 411-430, 2000.